Food and Chemical Toxicology 124 (2019) 239–248

Contents lists available at ScienceDirect

Food and Chemical Toxicology

journal homepage: www.elsevier.com/locate/foodchemtox

The cytotoxicity activity of *Hohenbuehelia serotina* polyphenols on HeLa cells via induction of cell apoptosis and cell cycle arrest

Lu Wang[a], Xiaoyu Li[a,*], Binbin Wang[b]

[a] School of Environmental and Chemical Engineering, Yanshan University, Qinhuangdao, 066004, PR China
[b] School of Materials Science and Engineering, Harbin Institute of Technology, Harbin, 150090, PR China

ARTICLE INFO

Keywords:
Polyphenols
Chemical composition
Anti-neoplasm activity
Apoptosis
Cell cycle

ABSTRACT

Hohenbuehelia serotina, is not only one important source of polysaccharides but also a good origin of polyphenols with antineoplastic functions in non-clinical researches. In this study, the polyphenols from *H. serotina* (HSP) were mainly composed by caffeic acid dimer, (−)-epicatechin-3-(3′-o-methyl)-gallic acid dimer, quercetin-acetyl-rutinoside hexoside, (−)-epigallocatechin derivatives, rutin derivatives, catechin trimer and 3-caffeoyl-quinic acid. HSP significantly inhibited the proliferation of HeLa cells *in vitro*, and induced intracellular ROS accumulation. It was also observed that induction of HeLa cells apoptosis and termination of cell cycle at G0/G1 phase were associated with the anti-tumor activity of HSP. On the basis of the expanded investigations of anti-neoplasm mechanism, HSP could decrease the mRNA expressions of cell cycle related genes including cyclin D1, Ckd2 and Cdk4, and increase the mRNA expressions of p53 and p21. In addition, the mitochondrial apoptosis pathway in HeLa cells was initiated by HSP through activation of Bax, cytochrome *c* and Caspase-3, as well as inhibition of Bcl-2. This study might provide a theoretical basis for the application of *H. serotina* polyphenols as tumor preventive agent.

1. Introduction

Mushroom is an important edible resource for human with a long history. In the ancient time of China, people did not only use the mushroom as the food material, but also for curing the sickness (Feng et al., 2016). According to Compendium of Materia Medica, mushroom possesses the anti-decrepitude function that could strengthen the body with long term intake (Luo et al., 2009; Liu et al., 2016). Nowadays, it is used for the medicinal and edible material approved by China Food and Drug Administration (CFDA). Therefore, mushroom has been attracted more attention due to their biological and pharmacological effects (Pluchino et al., 2015; Stojković et al., 2017). Almost all of the literature had focused on the polysaccharides in mushroom as the major bioactive compounds, and as well as a small amount of nucleotides (Liu et al., 2014; Meng et al., 2016). However, little attention was devoted on the other constituents of mushroom, such as polyphenols, proteins, pigments and etc, which might have various functional activities as well (Hwang et al., 2015; Ismaya et al., 2016; Prados-Rosales et al., 2015). Therefore, the exploration of new bioactive components in mushroom appears extremely important.

Tumor, which defines as the most fatal disease for human body, is difficult to completely cure in nowadays (Ammar et al., 2016). With the deterioration of the living environment, such as smog, chemical pesticides, automobile exhaust, industrial waste water and gas, and the increase of life pressure, the incidence of tumor presents a rising trend year by year. Among all the neoplasms, cervical carcinoma is one of the most common diseases. The research found that the occurrence of cervix was closely correlated to viral infection, sexual behavior, the number of parturitions, and unhealthy lifestyle (Xie et al., 2017). Once the normal cell cancerated, the neoplasm fast turned into a complicated and multistep tumor metastasis process, leading to the initiation of surrounding tissues invasion (Braster et al., 2017). At present, chemotherapy and radiotherapy have been widely used in the treatment of various tumors. However, due to the autoimmune response and immune tolerance, the treatments unavoidably brought some severe adverse effects, such as nausea and vomiting, hyperpyrexia, alopecia, stomatitis and etc (Wang et al., 2013). Therefore, the therapy based on the healthy and functional food becomes more important and popular. Polyphenolic compounds are the main secondary metabolites in natural plants and fungi (Carito et al., 2017). Many *in vivo* and *in vitro* studies showed that polyphenols possessed the significant inhibitory effect on tumor growth, exerting the adjuvant for cancer therapies. Rocha-Guzmán et al. (2009) reported that the phenolic compounds from *Quercus resinosa* leaves possessed the significant inhibitory activity on

* Corresponding author.
E-mail addresses: wl@ysu.edu.cn (L. Wang), lixiaoyu@ysu.edu.cn (X. Li), wl1986004@126.com (B. Wang).

https://doi.org/10.1016/j.fct.2018.12.001
Received 20 September 2018; Received in revised form 14 November 2018; Accepted 3 December 2018
Available online 07 December 2018
0278-6915/

viability of HeLa cells through genotoxic effect. Subsequently, the anti-proliferation functions of polyphenols were further confirmed by Kchaou et al. (2016). Pires et al. (2018) proved that the suppression of HeLa cell proliferation was intimately associated with the phenolic compositions. On the basis of structure-activity relationship analysis, the functional hydroxyl groups contributed to the excellent biological activities of polyphenols through donation of electrons or hydrogen atoms (Lewandowska et al., 2016). However, the anti-proliferation effect of mushroom polyphenols is still rarely reported.

Previously, we have investigated the significant bioactivities of *H. serotina* polysaccharides including antioxidant, immunomodulation, anti-cancer and radioprotective effects. In China, *H. serotina*, belongs to *Pleurotaceae*, is widely distributed in the northeast region, especially in Heilongjiang Province. *H. serotina* is consumed as a kind of rare mushroom due to its good flavour and abundant nutrient compositions, such as polysaccharides, nucleotides, polyphenols, etc. Nevertheless, up to now, no investigation has ever been concentrated on the anti-proliferation of the polyphenols from *H. serotina*. Therefore, the objective of this study was to extract and purify the *H. serotina* polyphenols, identify the polyphenolic compositions through HPLC-ESI-MS/MS, and then reveal the inhibitory mechanism against the HeLa cell growth.

2. Material and method

2.1. Materials and chemicals

H. serotina mushroom was purchased from a local market. The mushroom was produced in Shangzhi, Heilongjiang Province, China. The voucher specimen was characterized by Professor Zhenyu Wang, School of Chemistry and Chemical Engineering, Harbin Institute of Technology, China. 2, 2-azino-bis-(3-ethyl-benzthia-6-sulfonic acid) (ABTS), dimethyl sulfoxide, ascorbic acid were bought from Sigma-Aldrich (St. Louis, USA). The kits of mitochondrial apoptosis proteins (Bax, Bcl-2, cytochrome *c* and Caspase-3) were purchased from Nanjing Jiancheng Bioengineering Institute (Nanjing, China). All other reagents were of analytical grade.

2.2. Preparation of H. serotina polyphenols (HSP)

Mushroom was powdered through 60 mesh. The extraction process of HSP was performed according to the method of Wang et al. (2016b) with some modifications. Briefly, 10 g of the dried mushroom powder was extracted with 60% alcohol aqueous solution in a ratio of 1:20 (g/mL). The mixture was treated with the ultrasonication at 50 °C for 30 min, and then centrifuged at 4000 rpm for 10 min. The supernatant was collected, and the precipitate was reextracted for another two times by the method as mentioned above. The extraction yield was 0.62 ± 0.08% by measurement of Folin-ciocalteu method with gallic acid as standard. After the isolation process, the fraction of supernatant was mixed, and concentrated under the vacuum condition. Crude polyphenolic extracts were obtained, and then separated by macroporous resin AB-8 column chromatography. The elution process was employed by 40% alcohol aqueous solution with the volume of 2 BV. Then the elution with the purity of 99.47 ± 0.74% was concentrated, lyophilized and then stored at 4 °C for further research.

2.3. Compositional analysis of the polyphenolic compounds by HPLC-ESI-MS/MS

The phenolic compounds presented in *H. serotina* were identified by HPLC-ESI-MS/MS analysis. The instrument was conducted on Agilent 1290 HPLC coupled to an Agilent triple-quadruple mass-selective detector (Agilent Technologies, Waldbronn, Germany). The sample (20 μL) was injected into a reversed phase Agilent Symmetry C18 column. The mobile phase was composed of 0.1% formic acid aqueous solution (solvent A) and methanol (solvent B) with in a linear gradient. The condition of chromatographic was performed as follows: 2.0 min with 80% A + 20% B; 4.0 min with 60% A + 40% B; 6.0 min with 40% A + 60% B; 8.0 min with 40% A + 60% B; 10.0 min with 10% A + 90% B; 15 min with 10% A + 90% B. Mass spectrometer was equipped with an ESI ion source operating in MS/MS positive mode with the condition of The mass range explored was 100–1000 *m/z*.

2.4. Fourier transform-infrared spectroscopic analysis (FT-IR)

The FT-IR spectrum of HSP was carried out using FT-IR spectrometer (Thermo Co., USA) through KBr pellet method in a wavelength range of 4000–400 cm^{-1}.

2.5. X-ray diffraction

The crystalline structure of HSP was analyzed by an X-ray diffractometer (Rigaku Inc., Tokyo, Japan). The sample was equilibrated for 24 h under the condition of room temperature, and then measured according to the following parameters: Cu Kα radiation, 40 kV, 200 mA, the scanning range of 5–90° with the scan rate of 0.5°/min.

2.6. Morphology analysis

The microstructure configuration of HSP was analyzed by scanning electron microscopy (SEM). The sample was sputtered and coated with vacuum spray gold. Then, field emission scanning electron microscopy (SUPRA 55, ZEISS Co., Germany) was implied to observe the morphology of HSP.

2.7. Anti-proliferation effect of HSP on HeLa cell in vitro

2.7.1. Cell viability and morphology assay

The cell viability was performed by MTT method. Briefly, the cell was cultured in RPMI 1640 with 10% fetal bovine serum, 100 IU/mL of penicillin and 100 μg/mL of streptomycin. Then the cell (2×10^5 cells/well) was seeded into 96-well plates, and respectively treated with different concentration (0, 10, 20, 30, 40, 50 μg/mL) of HSP for 48 h. After the incubation, 20 μL of MTT was added to form formazan crystals, and then dissolved by 100 μL of DMSO. The absorbance of the mixture was measured at 570 nm using a microplate reader (Spectra Max M2e, Molecular Devices CO., USA). The morphological alternations of HeLa cells treated with different concentration of HSP were observed by inverted fluorescence microscope (LWD300-38LFT, Shanghai, China). In order to test the anti-proliferation effect of HSP on other cancer cells, human colon carcinoma HCT116 cells were used to incubate with different concentration of HSP, and the viabilities were analyzed by MTT method.

2.7.2. Cytotoxicity analysis

The cytotoxicity of HSP was performed on the viabilities of uterine cervical fibroblasts. The uterine cervical fibroblasts were isolated from the normal and healthy cervical tissue in mice. Briefly, the specific pathogen-free mouse was bred on a 12 h dark/12 h light cycle at 22 ± 2 °C. The mouse was sacrificed by cervical dislocation. The uterine cervical was quickly collected and washed by PBS buffer solution under sterile condition. After that, the uterine cervical was moderately scarped by sterile scalpel, and the uterine cervical fibroblasts were obtained. The isolated cells were incubated in DMEM media containing 10% fetal bovine serum, 100 IU/mL of penicillin and 100 μg/mL of streptomycin. The effect of HSP on viabilities of uterine cervical fibroblasts was measured by MTT methods, as mentioned above.

2.7.3. Measurement of intracellular ROS level

ROS level was analyzed by monitoring the fluorescent intensity of DCF, which was produced from oxidation of DCFH-DH by ROS. The

HeLa cells were incubated in a 12-well plate with different concentration of HSP at 37 °C under a humidified atmosphere containing 5% carbon dioxide. After incubation of 48 h, the cells were harvested, and washed by PBS for twice. The cells were continued to incubate with 10 μM DCFH-DH at 37 °C for 1 h. The fluorescent intensity was detected at an excitation wavenumber of 485 nm, and an emission wavenumber of 525 nm.

2.7.4. Cell cycle distribution analysis

The HeLa cells were treated as mentioned above. After cleaning by PBS, the cells were resuspended and fixed with cold 70% ethanol for overnight at 4 °C. The sample was subsequently subjected to PI labelling (PI/RNase Staining Buffer), and then the cell cycle was analyzed by flow cytometer (FACS Calibur, BD).

2.7.5. Cell apoptosis assay

The apoptosis-associated changes of HeLa cells were measured by flow cytometer using Annexin V-FITC cell apoptosis kit. Briefly, the cells were treated as the method described above. After the treatment, the cells were labelled with PI and Annexin V-FITC for 10 min at room temperature in the dark. Finally, the apoptosis cells were analyzed by flow cytometer (FACS Calibur, BD).

2.7.6. ELISA assay

The HeLa cells were incubated at the same condition as mentioned above. The protein expression (Bax, Bcl-2, cytochrome *c* and Caspase-3, Nanjing Jiancheng Bioengineering Institute, Nanjing, China) in HeLa cells treated with different concentration of HSP (0, 10, 30 and 50 μg/mL) was determined by ELISA method according to the instruction of kit.

2.7.7. Real-time qPCR assay

HeLa cells were administrated with different concentration of HSP (0, 10, 30 and 50 μg/mL) for 48 h. The total RNA was isolated from HeLa cells by TRIzol reagent. Then, reverse-transcription reaction was performed to synthesize first-strand cDNA for real-time qPCR reaction. SYBR Green was carried out to detect the dsDNA products during the real-time qPCR reaction. The reaction was repeated in triple. The specific primer sequences were exhibited in Table 1.

2.8. Statistical analysis

All the values were expressed as means ± SD (n = 3). Statistical analysis was performed by one-way analysis of variance (ANOVA) using SPSS (version 16.0). Differences at $p < 0.05$ and $p < 0.01$ were considered statistically significant by Duncan's new multiple-range test.

Table 1
The sequence of primer used in RT-PCR.

Gene	Primer	Sequence (5′-3′)
Bax	Forward	AGTAACATGGAGCTGCAGAGG
	Reverse	ATGGTTCTGATCAGTTCCGG
Bcl-2	Forward	GGAGCGTCAACAGGGAGATG
	Reverse	GATGCCGGTTCAGGTACTCAG
Cytochrome *c*	Forward	CCTCTGGGGCATTATCCATC
	Reverse	ATATTTGCACAGTGAAACATAGGA
Caspase-3	Forward	TGGACTGTGGCATTGAGACA
	Reverse	CAGGTGCTGTGGAGTATGCA
p53	Forward	CCTCAGCATCTTATCCGAGTGG
	Reverse	TGGATGGTGGTACAGTCAGAGG
p21	Forward	GCGGAACAAGGAGTCAGACA
	Reverse	GAACCAGGACACATGGGGAG
Cyclin D1	Forward	ATGGAACACCAGCTCCTGTGCTGC
	Reverse	TCAGATGTCCACGTCCCGCACGT
Cdk2	Forward	CCTGCTTATCAATGCAGAGGG
	Reverse	TGCGGGTCACCATTTCAGC
Cdk4	Forward	ATGGCTGCCACTCGATATGAA
	Reverse	TCCTCCATTAGGAACTCTCACAC
β-actin	Forward	GAACCAGGAGTTAAGAACACG
	Reverse	AGGCAACAGTGTCAGAGTCC

3. Results and discussion

3.1. FT-IR spectrum of HSP

Fig. 1a showed the FT-IR spectrum of HSP through KBr pellet method. The broad band at 3400 cm^{-1} in the FT-IR spectra was mainly assigned to the stretching vibration of O—H bonds derived from the phenolic structure (Zhang et al., 2017a). The peaks in the region of 2952–2920 cm^{-1} were attributed to the stretching vibration of C—H bonds, which was the characterized aromatic structure. The peak around 1560 cm^{-1} was considered as the presence of phenolic components. Especially, the peaks at 1318 cm^{-1} and 1260 cm^{-1} were belonged to the stretching vibration of phenyl–OH structure, which was also recognized as the characteristic groups in polyphenols (Pawlaczyk-Graja et al., 2016). The results described as above suggested HSP possessed the characteristic groups of polyphenols.

3.2. X-ray diffractogram of HSP

X-ray diffractometer was performed to investigate the crystalline property of HSP. The spectrum of X-ray diffractogram was recorded in the range of 5–90°, as shown in Fig. 1b. The result suggested that the nature of HSP tended to be semi-crystalline with the “bun” shape of crystalline reflection at 21°. The crystalline property plays an important role in the physicochemical characteristics, such as solubility, swelling and viscosity, which directly affect the development and application of natural products in health food field (Ktari et al., 2017).

3.3. Morphological observation

The scanning electron micrograph (SEM) of HSP was exhibited in Fig. 1c. HSP possessed the relative smooth surface with lump clusters. The clusters linked with each other. In addition, there were some uniform holes on the micro-structural surface of HSP. The reason might be due to that the polyphenols stablely existed in the form of phenolic-glycosides, leading to molecular crosslinking (see Table 2).

3.4. Phenolic composition of HSP

In order to identify the composition of *H. serotina* polyphenols, HPLC-ESI-MS/MS was conducted to characterize these compounds. Table 1 exhibited the retention time, MS and inferred characterization results of the phenolic compounds. On the basis of mass measurement of molecular ions and subsequent fragment ions, as well as the reference of ESI-MS and MS/MS data in the literature (Zhang et al., 2015, 2017b; Hsu et al., 2017; Wang et al., 2008; Xie et al., 2011; Vallverdú-Queralt et al., 2015; Papetti et al., 2017), the compositions of polyphenols in *H. serotina* extract were tentatively identified, mainly including caffeic acid dimer, (−)-epicatechin-3-(3′-o-methyl)-gallic acid dimer, quercetin-acetyl- rutinoside hexoside, (−)-epigallocatechin derivatives, rutin derivatives, catechin trimer and 3-caffeoylquinic acid.

3.5. Anti-proliferative effect of HSP on HeLa cell in vitro

3.5.1. Cell viabilities

The anti-proliferative effect of HSP on HeLa cells was measured by cytotoxic MTT assay. As shown in Fig. 2a, the cell viabilities were inhibited by administration with HSP in a dose-dependent manner. When the concentration of HSP was 50 μg/mL, the inhibitory rate on HeLa cell viability reached to 45.04 ± 1.52%. The result suggested that HSP played an important cytotoxic role in the survival of HeLa cells. In order to evaluate the anti-neoplasm effect of HSP on other tumor cells, the

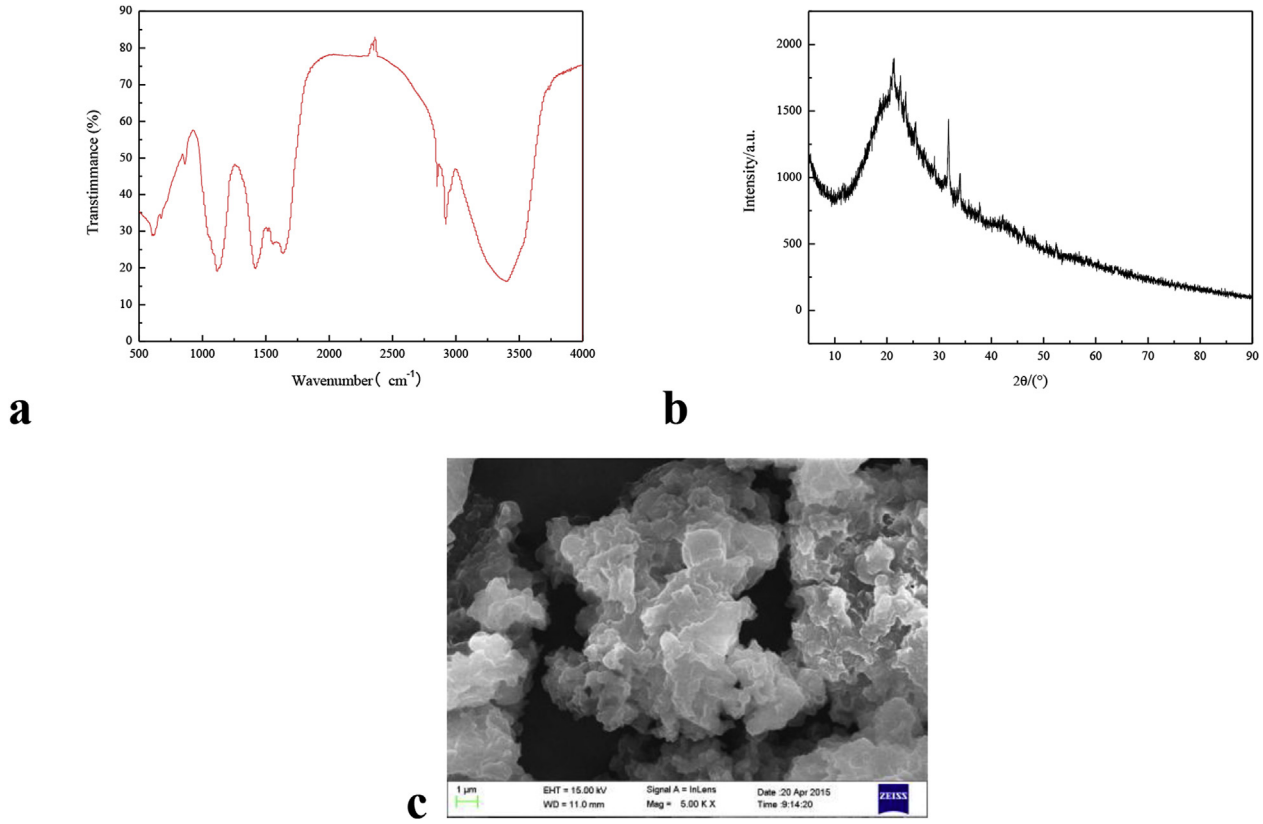

Fig. 1. Structural characteristics and morphology of HSP (a: X-ray diffraction spectrum; b: FT-IR spectrum; c: SEM image).

inhibitory activity of HSP on viabilities of HCT116 cells were also measured. The result exhibited that HSP possessed the similar anti-proliferation function on HCT116 as HeLa cells, suggesting that HSP had the bright potential to be served as natural food anticancer agent.

3.5.2. Cell morphology

The morphology of HeLa cells treated with HSP for 48 h was observed, and the images were exhibited in Fig. 3. The density of HeLa cells was decreased in a dose-dependent manner. Moreover, the HeLa cells exposed to different concentration of HSP showed the abnormal morphologies. The cells were transformed to round shape, and peeled off from the wall of cell culture flask, as well as turned to shrink. The result showed that administration with HSP significantly influenced the morphology of HeLa cells.

3.5.3. Cytotoxicity

As the natural anticancer agent, HSP must have no toxic and side effects on normal tissue or cells. Therefore, the cytotoxicity of HSP on fibroblasts from uterine cervical of mice was investigated, as shown in Fig. 2b. After treatment with different concentration of HSP, the viabilities of fibroblasts did not change significantly, indicating that HSP did not exhibited the toxic and side effects on growth of fibroblasts within the experimental concentration range. The result also illustrated that HSP might be served as a potential therapeutic agent for cancer.

3.5.4. Intracellular ROS level

Fig. 2c showed the ROS content in HeLa cells administrated with different concentration of HSP. The level of ROS was increased in a concentration-dependent manner. Furthermore, the ROS content in the 50 μg/mL of HSP treated group was significantly far higher that the non-treated group ($p < 0.01$). Above result suggested that HSP could induce ROS accumulation in HeLa cells.

3.5.5. Apoptosis

Flow cytometry with Annexin-V/PI double staining was performed to measure the effect of HSP on HeLa cell early/late apoptosis or necrosis, as shown in Fig. 4. As a whole, early apoptosis cells increased after treatment with HSP for 48 h in a dose-dependent manner. In comparison with the non-administration group (4.66%), at the concentration of 50 μg/mL, HSP exerted the inductive function on early apoptosis of HeLa cells with the value of 7.11%. However, the proportion of HeLa cells in late apoptosis or necrosis state significant increased from 5.10% to 9.16%, and the total quantities of apoptosis and necrosis cells were significantly increased after treatment with HSP.

Table 2
Composition of monomers in HSP.

No.	Retention time (min)	m/z [M+H]+	err (mDa)	Fragments	Proposed compound
1	6.0	792.6	−1.56	396.9	Caffeic acid dimer
2	6.3	905.7	−0.20	453.4	(−)-Epicatechin-3-(3′−O-methyl)-gallic acid dimer
3	9.7	814.5	−1.20	299.2	Quercetin-acetyl-rutinoside hexoside
4	10.3	814.5	0.12	149.1/301.2	(−)-Epigallocatechin derivatives
5	10.8	814.4	−0.71	299.1	Rutin derivatives
6	11.2	814.5	−0.65	289.3	Catechin trimer
7	11.8	814.6	1.40	303.3/353.3	3-Caffeoylquinic acid

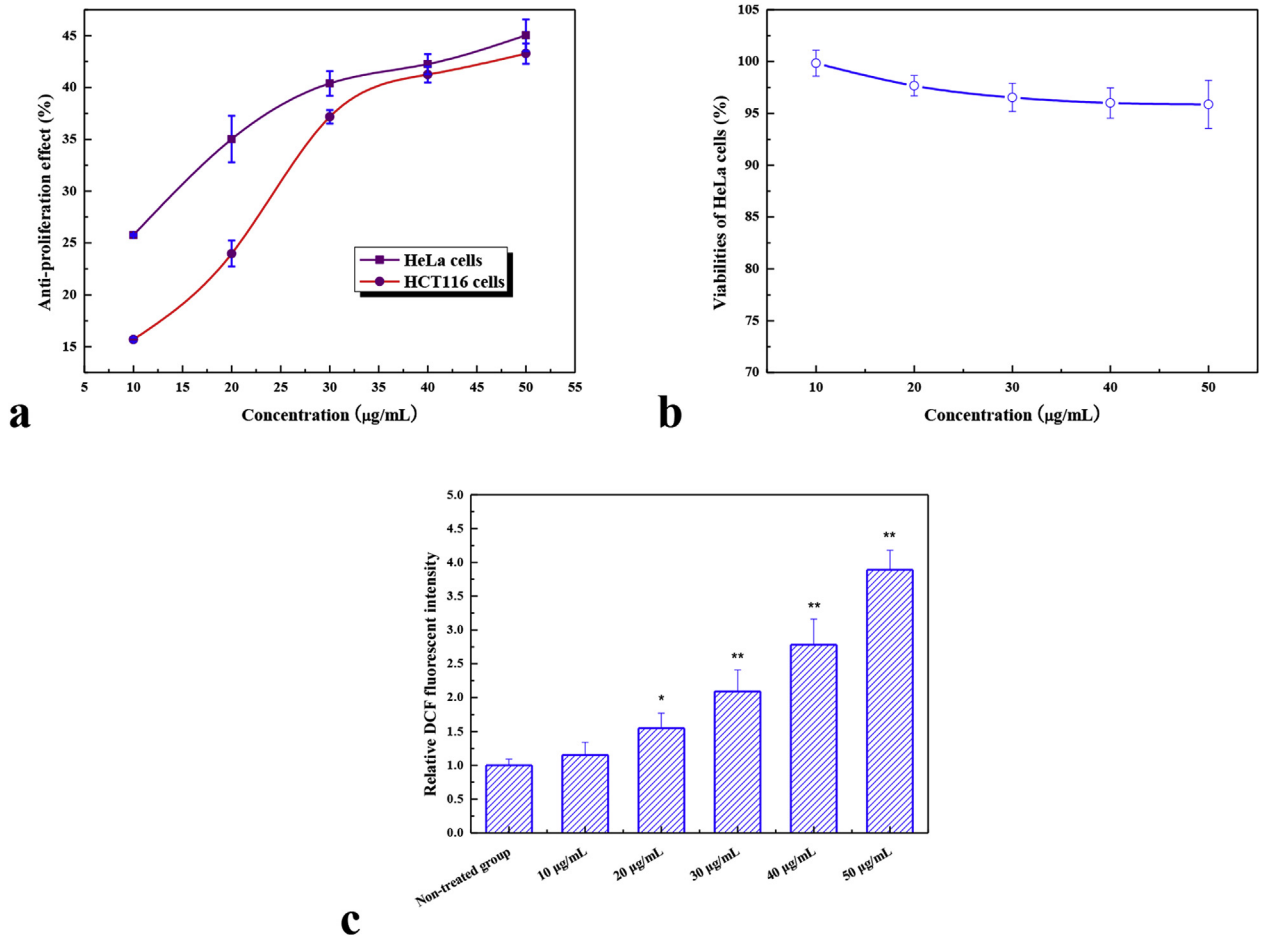

Fig. 2. The effects of HSP on (a) the viabilities of HeLa cells and HCT116 cells by MTT method, (b) the viabilities of fibroblasts from uterine cervical of mice and (c) ROS level in HeLa cells. The ROS level in HeLa cells was measured after treated with different concentration (10, 30 and 50 μg/mL) of HSP for 48 h * vs. non-treated group, $p < 0.05$; ** vs. non-treated group, $p < 0.01$.

3.5.6. Cell cycle

To investigate the reason of HeLa cell apoptosis induced by HSP, cell cycle was measured using flow cytometry. As shown in Fig. 5, HSP significantly inhibited the physiological differentiation process of HeLa cells, and induced the cells accumulation in G0/G1 phase compared with non-treatment group, while the amounts of cells in S and G2/M phases were correspondingly decreased in dose dependent manner. Compared to non-treated group (26.72%), at the concentration of 50 μg/mL, the number of HeLa cells arrested at G0/G1 phase was the most, with the value of 45.34%.

3.5.7. Expression of apoptosis protein in mitochondrial pathway

The effects of HSP on the activity of Bax, Bcl-2, cytochrome *c* and Caspase-3 in HeLa cells were respectively investigated, as shown in Fig. 6. The result clearly showed that administration with HSP could increase the expressions of Bax, cytochrome *c* and Caspase-3 in a dose-

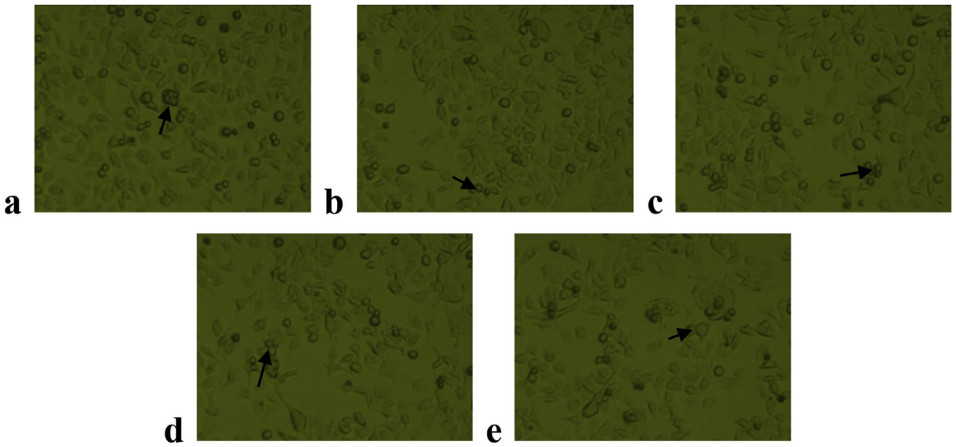

Fig. 3. The morphology of HeLa cell treated different concentration of HSP for 48 h (a–e: 10, 20, 30, 40, 50 μg/mL) *in vitro*. The images were observed by an inverted fluorescence microscope. The arrows represent the apoptosis bodies.

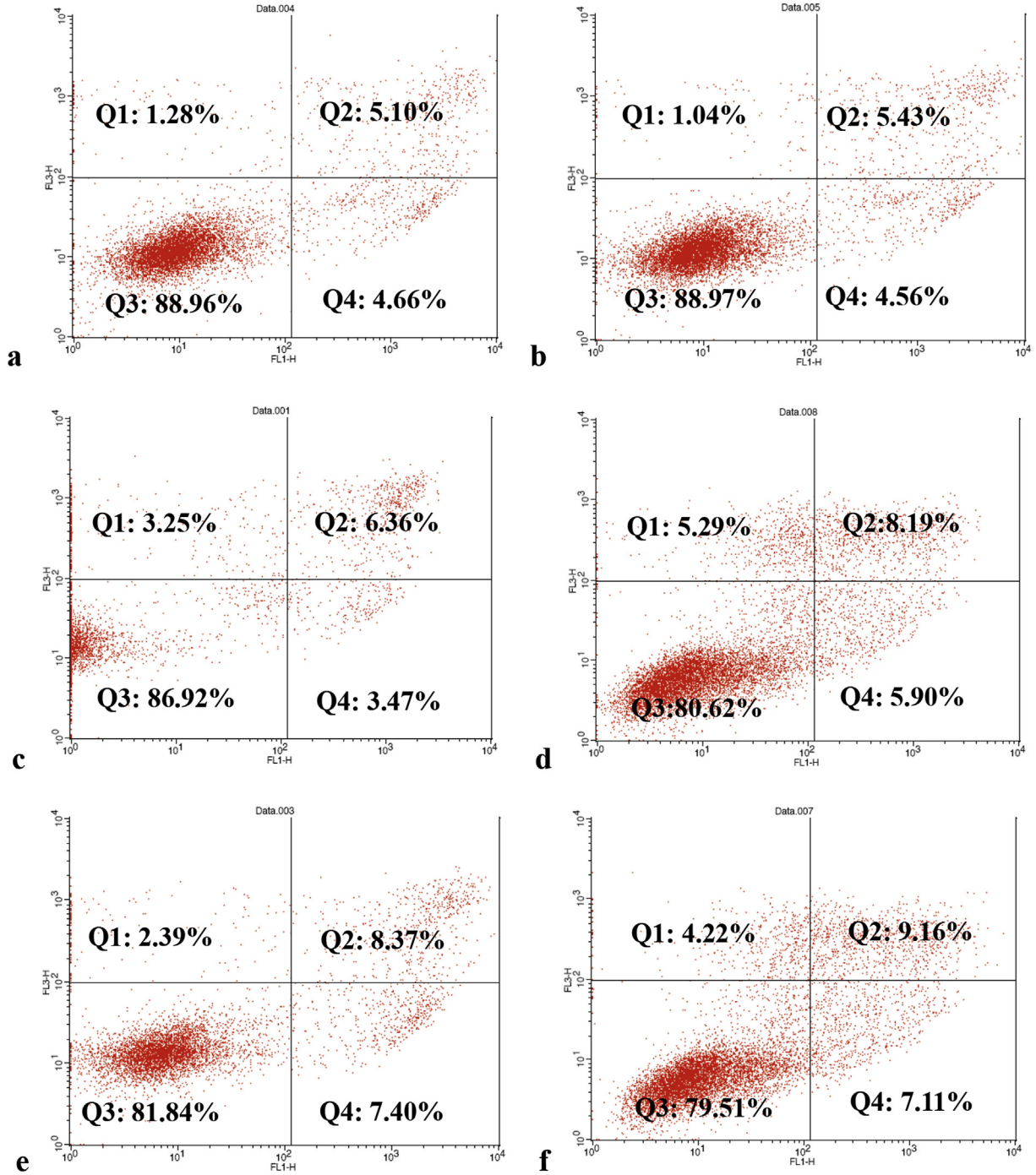

Fig. 4. The late apoptosis of HeLa cell induced by HSP through analysis of Annexin V FI-TC and PI staining. a: HeLa cells without any treatment; b: HeLa cells with treatment of 10 μg/mL HSP; c: HeLa cells with treatment of 20 μg/mL HSP; d: HeLa cells with treatment of 30 μg/mL HSP; e: HeLa cells with treatment of 40 μg/mL HSP; f: HeLa cells with treatment of 50 μg/mL HSP.

dependent manner. However, the expression of Bcl-2 was correspondingly decreased by administration with HSP. Our results showed that the mitochondrial apoptosis pathway was initiated by HSP in HeLa cells.

3.5.8. The mRNA expression of mitochondrial apoptosis pathway related gene

To further elucidate the anti-neoplasm effect of HSP through mitochondrial pathway *in vitro*, the mRNA expression was measured by RT-qPCR reaction. As shown in Fig. 7, among all three individual administrations, the mRNA expression levels of Bax, cytochrome *c* and Caspase-3 were all increased at different degrees. However, the mRNA expression content of Bcl-2 was correspondingly decreased.

3.5.9. The mRNA expression of cell cycle related gene

Since G0/G1 phase arrest was observed in HeLa cell treated with different concentration of HSP, efforts were made to elucidate whether HSP influenced the mRNA expression of related gene including p53, p21, Cyclin D1, Cdk2 and CDK4. Fig. 8 showed that the mRNA expressions of p53, p21, Cyclin D1, Cdk2 and CDK4 were all elevated by administration with HSP for 48 h in comparison with the non-treated control, suggestion that HSP played an important role in induction of

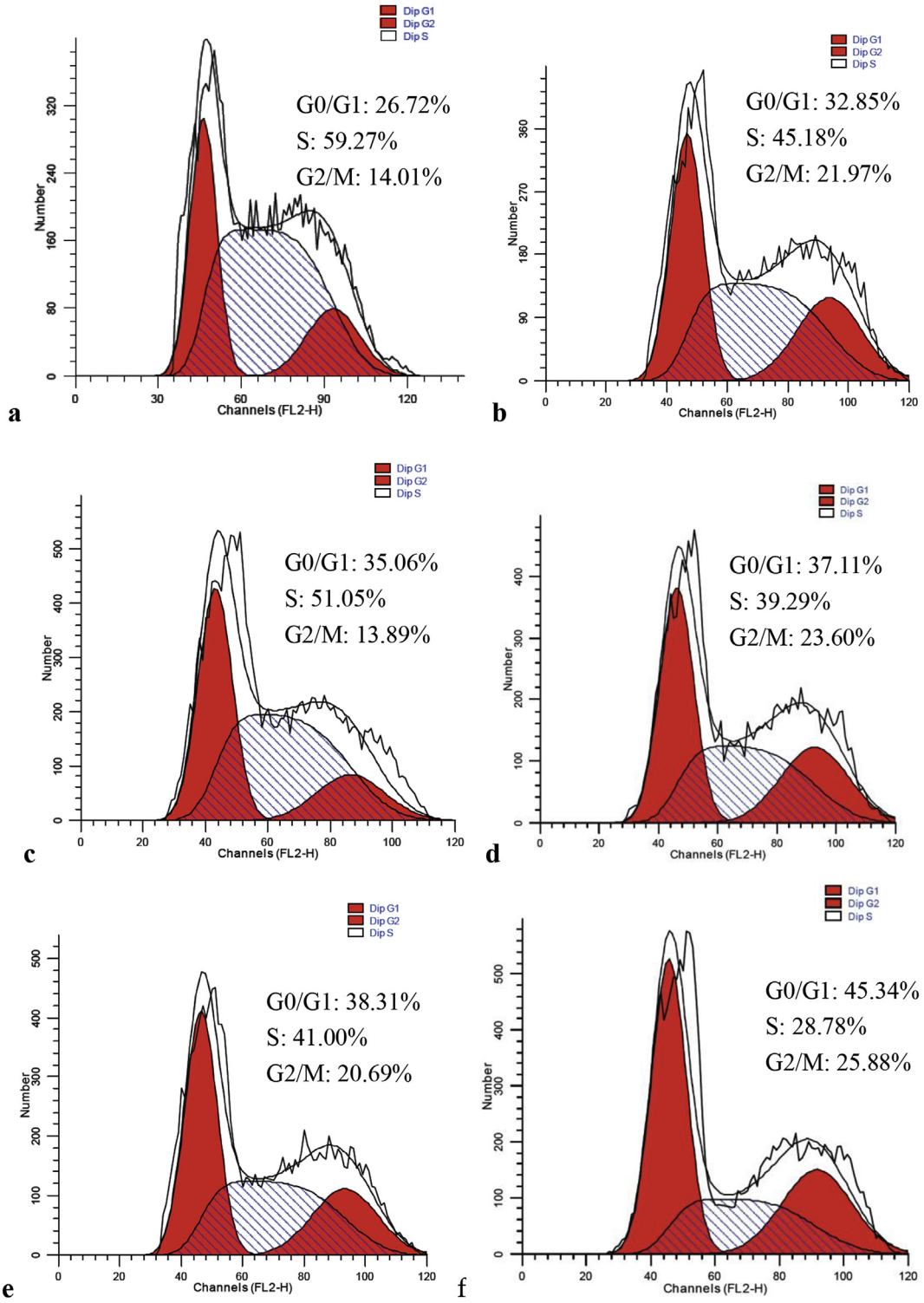

Fig. 5. The effect of HSP on HeLa cell cycle arrest. a: HeLa cells without any treatment; b: HeLa cells with treatment of 10 μg/mL HSP; c: HeLa cells with treatment of 20 μg/mL HSP; d: HeLa cells with treatment of 30 μg/mL HSP; e: HeLa cells with treatment of 40 μg/mL HSP; f: HeLa cells with treatment of 50 μg/mL HSP.

cell cycle arrest at G0/G1 phase.

4. Discussion

Nowadays, polysaccharides have been regarded as the main functional constituents in mushrooms due to multiple biological and pharmacological activities, such as immunomodulation, antioxidant, antitumor, radioprotection, hypoglycemic and etc (Ruthes et al., 2016; Li and Wang, 2016). Nevertheless, the other active ingredients in mushrooms are generally ignored. In recent years, the researchers gradually found that the polyphenols isolated from mushrooms also possessed kinds of bioactive effects. For instance, Hwang et al. (2015) investigated the anti-influenza activities of polyphenols from the mushroom *Phellinus baumii*; Jaworska et al. (2014) found that the phenolics isolated from *Suillus luteus* (L.) Roussel mushroom possessed the significant antioxidant activities; Kaewnarin et al. (2016) discovered that

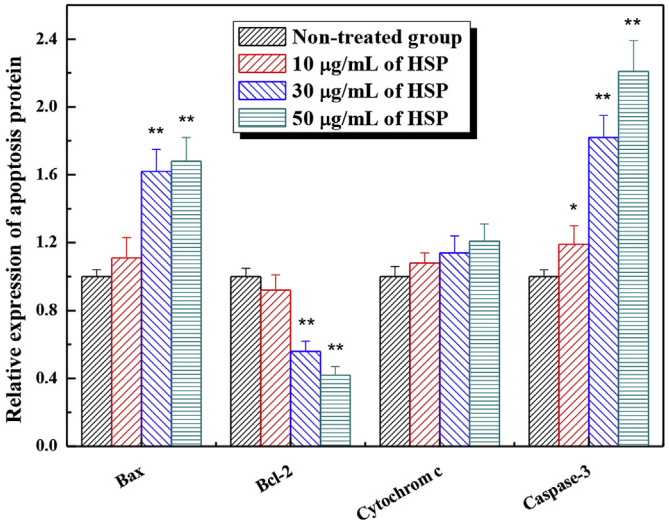

Fig. 6. The expressions of mitochondrial apoptosis pathway related protein in HSP treated HeLa cells. The protein expression was measured after treated with different concentration (10, 30 and 50 μg/mL) of HSP for 48 h by ELISA methods. * vs. non-treated group, $p < 0.05$; ** vs. non-treated group, $p < 0.01$.

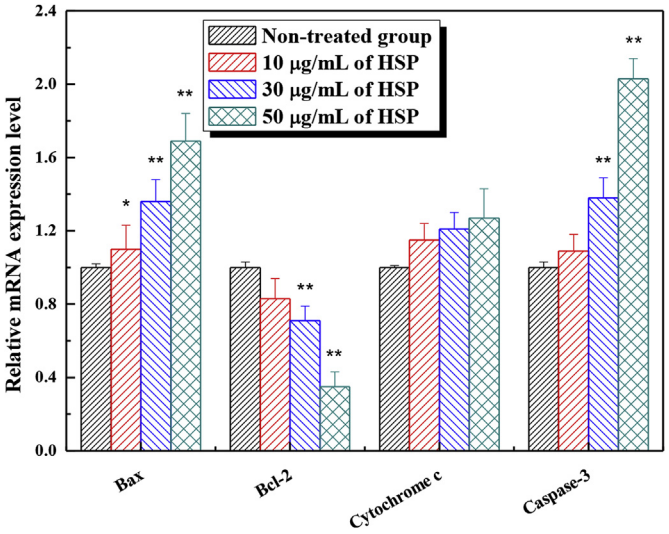

Fig. 7. The mRNA expression profile of mitochondrial apoptosis pathway related genes in HSP treated HeLa cells. The mRNA expression of related gene was measured after treated with different concentration (10, 30 and 50 μg/mL) of HSP for 48 h * vs. non-treated group, $p < 0.05$; ** vs. non-treated group, $p < 0.01$.

the phenolic compounds from various edible mushrooms (*Rugiboletus extremiorientalis*, *Russula emetica*, *Russula* sp. and *Phlebopus portentosus*) had the excellent antioxidant, anti-tyrosinase and hyperglycaemic inhibitory activities; Nowacka et al. (2014) investigated and found that the phenolic constituents from edible mushrooms possessed the remarkable antimicrobial activity. However, only a small amount of research is concentrated on the anti-tumor effect of mushroom polyphenols. Liu et al. (2017) isolated the phenolic compounds from mushroom *Inonotus sanghuang*, and investigated the antiproliferative activity of the phenolics. They found that the phenolics from *Inonotus sanghuang* exhibited the strongest antiproliferative effect against tumor cell PC3. Until now, the research on the anti-tumor mechanism of mushroom polyphenols is still rarely reported.

H. serotina is a kind of precious mushroom distributed in northeast of China. *H. serotina* is abundant in nutrition substances, such as

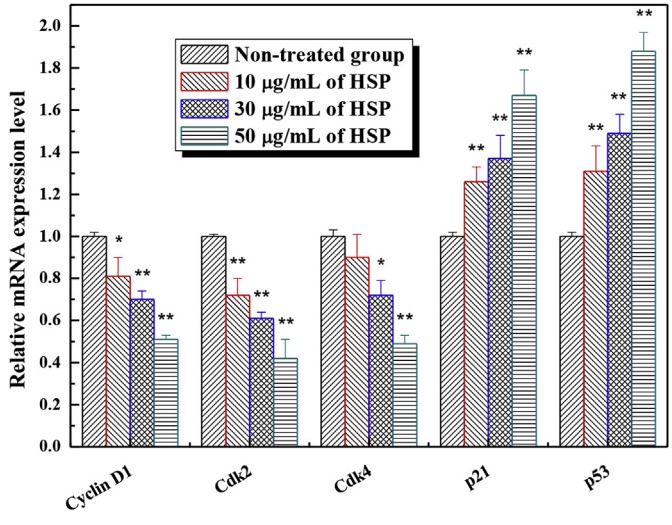

Fig. 8. The mRNA expression profile of G0/G1 phase regulatory related genes in HSP treated HeLa cells. The mRNA expression of related gene was measured after treated with different concentration (10, 30 and 50 μg/mL) of HSP for 48 h * vs. non-treated group, $p < 0.05$; ** vs. non-treated group, $p < 0.01$.

polysaccharides, proteins, nucleotides and polyphenols. We tentatively extracted the phenolic compounds from *H. serotina* by ultrasonic-assisted method, and then purified by macroporous resin AB-8 column chromatography to obtain the purified polyphenols (HSP). After characterization by HPLC-ESI-MS/MS, FT-IR, XRD and SEM, we found that HSP was a semi-crystalline substance, and possessed the relative smooth surface with lump clusters. HSP was mainly composed by caffeic acid dimer, (−)-epicatechin-3-(3′-o-methyl)-gallic acid dimer, quercetin-acetyl-rutinoside hexoside, (−)-epigallocatechin derivatives, rutin derivatives, catechin trimer and 3-caffeoylquinic acid.

The cytotoxicity effect of HSP on HeLa cells was comprehensively determined to elucidate the anticancer mechanism. HSP presented the significant inhibitory activity on viabilities of HeLa cells in dose-dependent manner, which was also demonstrated by the morphological alternations. According to literature, polyphenols including resveratrol, quercetin, and catechin possessed the similar remarkable inhibition on neoplasm cell proliferation (Omidian et al., 2017). The anti-proliferation effect might be associated with the induction of oxidative stress in neoplasm cells. Many researchers reported that oxidative stress induced by polyphenols through accumulation of reactive oxygen species (ROS), such as gallic acid, ellagic acid and procyanindin, contributed to apoptosis of cancer cells due to changing the intracellular microenvironment (González-Sarrías et al., 2017). Therefore, oxidative stress might be characterized as the main cause of cell apoptosis or necrosis.

ROS widely exists in the cells of living organisms, which is regarded as growth factors and intracellular signal molecules. ROS dose not only play an important role in energy metabolism but also in cell physiological processes (Wang et al., 2016a). Under the condition of harmful stimulation, excessive ROS is accumulated to induce oxidative stress in cell. Therefore, ROS accumulation is considered as one of the major targets for cancer treatment. As expected, our result found that HSP could obviously elevate the level of ROS in HeLa cells with dose dependent manner. Excessive production of ROS would directly result to cell apoptosis.

Apoptosis defines as the programmed cell death, which is a physiological process of cell. Induction of apoptosis is considered as the major pathway to inhibit the tumor cell proliferation by biological agents. This study suggested that the early and late apoptosis rate or necrosis rate was obviously increased by treatment with HSP compared with non-treated group. The apoptosis induction of HSP might be associated with the intracellular ROS levels in HeLa cells. Excessive ROS may interact with the biomembrane lipids, proteins and other

components, causing the oxidative damage. Apoptosis mainly divides into endogenous mitochondrial pathway and exogenous death receptor pathway, which all refer to a set of dormant proteases, such as Caspase family, which could cleave and activate the downstream apoptosis protein factors. The manifestation patterns of apoptosis mainly include cell shrinkage, mitochondrial depolarization, membrane rupture, DNA fragmentation and formation of apoptotic body (Wang et al., 2017). Growing evidence in cancer research by phenolic compounds suggested that mitochondrial pathway was regarded as the principal tumor suppressed pathway (Pal et al., 2016; Hsu et al., 2018). Bax and Bcl-2, both belong to Bcl-2 family, are respectively served as pro-apoptosis molecule and anti-apoptosis molecule in mitochondrial apoptosis pathway. In apoptosis process, Bax and Bcl-2 turn into binding with their receptors, leading to the changes of conformations. In addition, the ratio of Bax/Bcl-2 also changed seriously. Subsequently, the permeability of mitochondrial membrane is disrupted, resulting in the release of cytochrome *c* from mitochondrial to cytoplasm. Cytochrome *c* is a main constituent involving in electron transport, which can activate the expression of Caspase-3. Caspase-3 serves as the effector and executor in endogenous mitochondrial apoptotic pathway, which has crystal subunit, and possesses the pocket active site (Pandurangan et al., 2016). Once Caspase-3 is activated, the endogenous mitochondrial apoptosis process is switched on. In addition, the activated Caspase-3 is closely associated with the intracellular pH status and bioenergy metabolic in the cell (Sergeeva et al., 2017). Therefore, to further illustrate the apoptosis mechanism of HeLa cells induced by HSP, the expressions of mitochondrial related genes were analyzed by RT-qPCR. Our data found that HSP could effectively increase the mRNA expressions of Bax, cytochrome *c* and Caspase-3, as well as decrease the expression of Bcl-2 in HeLa cells, indicating that the endogenous mitochondrial apoptosis pathway was triggered by administration with HSP. Many literature reported that oxidative stress could be induced by polyphenols in cancer cells, leading to cell cycle disarrangement, mitochondrial dysfunction, DNA fracture, and ultimately apoptosis (Ma et al., 2017; Mondal and Bennett, 2016).

Cell cycle has a vital impact on regulation of cell physiology, such as cell proliferation and apoptosis. Therefore, cell cycle is regarded as central hinge to elucidate the anti-neoplasm mechanism (Liang et al., 2017). Therefore, next measurement was focused on the impact of HSP on HeLa cell cycle. The result showed that HSP caused an increase in the percentage of G0/G1 phase cells, leading to interdiction of cell physiological process. Cell cycle arrest of tumor cells induced by chemical intervention generally divides into two strategies: G1/S-phase arrest and G2/M-phase arrest (Wang et al., 2018). Accumulation of HeLa cells in G0/G1 phase by HSP contributed to the mediation of cell proliferation and apoptosis. Induction of apoptosis, arrest of cell cycle and inhibition of cell proliferation have been considered as the promising interventions on neoplasm, which were confirmed by our study (Chang et al., 2017). In order to further illuminate the regulatory mechanism, RT-qPCR analysis was performed to measure the mRNA expressions of cell cycle related genes. Cell cycle progression is controlled by cyclins, cyclin-dependent kinases (Cdks), and their complexes. Cdk2, Cdk4 and cyclin D1 are the three specific regulators in G0/G1 phase. Generally, Cdks are the binding partners of cyclin D, which are also activated by cyclin D to mediate the cell cycle progression (Yaguchi et al., 2018). Therefore, next issue was to detect the mRNA expressions of Cdk2, Cdk4 and cyclin D1 in HSP-treated HeLa cells. After treatment of HSP, the mRNA expressions of Cdk2, Cdk4 and cyclin D1 were all decreased at different degrees in dose-dependent manners, suggesting that HSP inhibited the activations of Cdk2, Cdk4 and cyclin D1 to induce the HeLa cells arrest at G0/G1 phase. As the inhibitor of Cdk, p21 could inhibit the formation of cyclin/Cdk complex. Once the expression of p21 is overwhelmed that will inhibit the activity of cyclin/Cdk complex, leading to cell cycle arrest (Xu and Kim, 2014). The p53 gene, described as the upstream regulator of p21, is a tumor suppressor, which is involved in regulation of cell cycle, DNA repair and apoptosis (Pereira et al., 2018). According to literature, p53 was associated with the activation of Bax in tumor cells (Wu and Shen, 2018). Through analysis of real time-qPCR, the mRNA expressions of p21 and p53 were significantly increased by administration of HSP in HeLa cells, suggesting that HSP triggered the expression of p53 to activate the upstream p21, and then regulated the activations of Cdk2, Cdk4 and cyclin D1, ultimately lead to G0/G1 phase block.

In summary, HSP belonged to semi-crystalline substances, and was mainly composed by caffeic acid dimer, (−)-epicatechin-3-(3′-o-methyl)-gallic acid dimer, quercetin-acetyl-rutinoside hexoside, (−)-epigallocatechin derivatives, rutin derivatives, catechin trimer and 3-caffeoylquinic acid. HSP significantly inhibited the growth of HeLa cells *in vitro*. HSP could induce HeLa cell arrest at G0/G1 phase by up-regulation of p53 and p21, and down-regulation of cyclin D1, Cdk2 and Cdk4. Furthermore, through activation of Bax, cytochrome *c* and Caspase-3, as well as inhibition of Bcl-2, the mitochondrial apoptosis pathway was induced by administration with HSP in HeLa cells. The core mechanism for anti-tumor effect of HSP included increase of intracellular ROS accumulation as initiate the apoptosis progression and termination of cell cycle at G0/G1 phase, ultimately leading to HeLa cells excessive apoptosis (Fig. 9). Our study supported a role for *H. serotina* polyphenols as natural protective agent against cervical carcinoma. However, the present research possessed certain limitations due to the experiments performed *in vitro*. Life body is an extremely complicated physiological system, hence, the anti-neoplasm activity of HSP need to be systemically investigated *in vivo*. So, the future research will be concentrated on the anti-tumor mechanism of HSP in *vivo* model.

Conflicts of interest

There are no conflicts to declare.

Acknowledgements

This research was supported financially by National Natural Science Foundation of China (31500652), Natural Science Foundation of Hebei Province (C2016203040) and Hebei Provincial Department of Education High School Science and Technology Plan Guidance Project (ZC2016053). The authors would like to thank Prof. Zhenyu Wang from the School of Chemistry and Chemical Engineering, Harbin Institute of technology, for helpful suggestions and assistance.

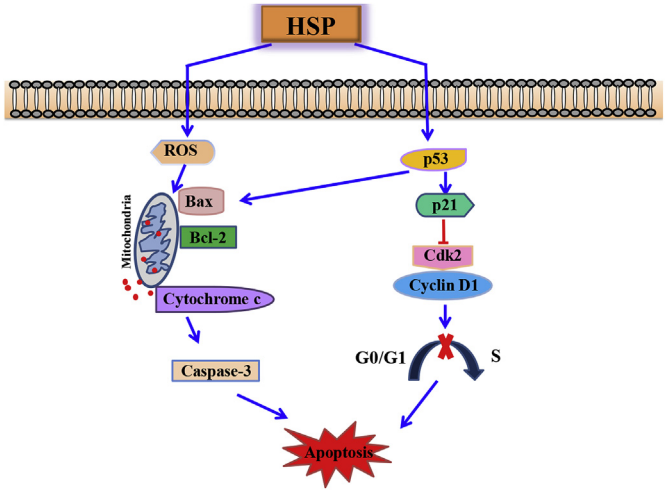

Fig. 9. Proposed anti-tumor mechanism of HSP on HeLa cells involving in cell cycle and apoptosis pathways.

Transparency document

Transparency document related to this article can be found online at https://doi.org/10.1016/j.fct.2018.12.001.

References

Ammar, A.A., Raveendran, R., Gibson, D., Nassar, T., Benita, B.A., 2016. Lipophilic Pt(IV) oxaliplatin derivative enhances antitumor activity. J. Med. Chem. 59, 9035–9046.

Braster, R., Bögels, M., Beelen, R.H.J., Egmond, M.V., 2017. The delicate balance of macrophages in colorectal caner; their role in tumour development and therapeutic potential. Immunobiology 222, 21–30.

Carito, V., Ceccanti, M., Cestari, V., Natella, F., Bello, C., Coccurello, R., et al., 2017. Olive polyphenol effects in a mouse model of chronic ethanol addiction. Nutrition 33, 65–69.

Chang, C., Korivi, M., Huang, H., Thiyagarajan, V., Lin, K., Huang, P., et al., 2017. Inhibition of ROS production, autophagy or apoptosis signalling reversed the anticancer properties of *Antrodia salmonea* in triple-negative breast cancer (MDA-MB-231) cells. Food Chem. Toxicol. 103, 1–17.

Feng, T., Cai, J., Li, X., Zhou, Z., Li, Z., Liu, J., 2016. Chemical constituents and their bioactivities of mushroom *Phellinus rhabarbarinus*. J. Agric. Food Chem. 64, 1945–1949.

González-Sarrías, A., Núñez-Sánchez, M.Á., Tomás-Barberán, F.A., Espín, J.C., 2017. Neuroprotective effects of bioavailable polyphenol-derived metabolites against oxidative stress-induced cytotoxicity in human neuroblastoma SH-SY5Y cells. J. Agric. Food Chem. 65, 752–758.

Hsu, B.Y., Lin, S.W., Inbaraj, B.S., Chen, B.H., 2017. Simultaneous determination of phenolic acids and flavonoids in *Chenopodium formosanum* Koidz. (djulis) by HPLC-DAD-ESI-MS/MS. J. Pharmaceut. Biomed. 132, 109–116.

Hsu, Y., Shyu, H., Hu, T., Yeh, J., Lin, Y., Lee, L., et al., 2018. Anti-proliferative activity of biochanin A in human osteosarcoma cells via mitochondrial-involved apoptosis. Food Chem. Toxicol. 112, 194–204.

Hwang, B.S., Lee, I., Choi, H.J., Yun, B., 2015. Anti-influenza activities of polyphenols from the medicinal mushroom *Phellinus baumii*. Bioorg. Med. Chem. Lett 25, 3256–3260.

Ismaya, W.T., Efthyani, A., Lai, X., Retnoningrum, D.S., Rachmawati, H., et al., 2016. A novel immune-tolerable and permeable lectin-like protein from mushroom *Agaricus bisporus*. Biochem. Biophy. Res. Co. 473, 1090–1093.

Jaworska, G., Pogoń, K., Bernaś, E., Skrzypczak, A., 2014. Vitamins, phenolic and antioxidant activity of culinary prepared *Suillus luteus* (L.) Roussel mushroom. LWT (Lebensm.-Wiss. & Technol.) 59, 701–706.

Kaewnarin, K., Suwannarach, N., Kumla, J., Lumyong, S., 2016. Phenolic profile of various wild edible mushroom extracts from Thailand and their antioxidant properties, anti-tyrosinase and hyperglycaemic inhibitory activities. J. Funct. Foods 27, 352–364.

Kchaou, W., Abbès, F., Mansour, R.B., Blecker, C., Attia, H., Besbes, S., 2016. Phenolic profile, antibacterial and cytotoxic properties of second grade date extract from Tunisian cultivars (*Phoenix dactylifera* L.). Food Chem. 194, 1048–1055.

Ktari, N., Feki, A., Trabelsi, I., Triki, M., Maalej, H., Slima, S.B., et al., 2017. Structure, functional and antioxidant properties in Tunisian beef sausage of a novel polysaccharide from *Trigonella foenum*-graecum seeds. Int. J. Biol. Macromol. 98, 169–181.

Lewandowska, U., Fichna, J., Gorlach, S., 2016. Enhancement of anticancer potential of polyphenols by covalent modifications. Biochem. Pharmacol. 109, 1–13.

Li, X., Wang, L., 2016. Effect of extraction method on structure and antioxidant activity of *Hohenbuehelia serotina* polysaccharides. Int. J. Biol. Macromol. 83, 270–276.

Liang, W., Jan, C., Hsu, S., 2017. Cytotoxic effects of gastrodin extracted from the rhizome of *Gastrodia elata Blume* in glioblastoma cells, but not in normal astrocytes, via the induction of oxidative stress-associated apoptosis that involved cell cycle arrest and p53 activation. Food Chem. Toxicol. 107, 280–292.

Liu, K., Xiao, X., Wang, J., Chen, C.-Y.O., Hu, H., 2017. Polyphenolic composition and antioxidant, antiproliferative, and antimicrobial activities of mushroom *Inonotus sanghuang*. LWT (Lebensm.-Wiss. & Technol.) 82, 154–161.

Liu, Y., Chen, D., You, Y., Zeng, S., Li, Y., Tang, Q., et al., 2016. Nutritional composition of boletus mushrooms from Southwest China and their antihyperglycemic and antioxidant activities. Food Chem. 211, 83–91.

Liu, Y., Huang, F., Yang, H., Ibrahim, S.A., Wang, Y., Huang, W., 2014. Effects of preservation methods on amino acids and 5'-nucleotides of *Agaricus bisporus* mushrooms. Food Chem. 149, 221–225.

Luo, Y., Chen, G., Li, B., Ji, B., Guo, Y., Tian, F., 2009. Evaluation of antioxidative and hypolipidemic properties of a novel functional diet formulation of *Auricularia auricula* and *Hawthorn*. Innov. Food Sci. Emerg. 10, 215–221.

Ma, S., Ju, F., Zhang, Y., Shi, X., Zhuang, R., Xue, H., et al., 2017. Cold-inducible protein RBM3 protects neuroblastoma cells from retinoic acid-induced apoptosis via AMPK, p38 and JNK signaling. J. Funct. Foods 35, 175–184.

Meng, X., Liang, H., Luo, L., 2016. Antitumor polysaccharides from mushrooms: a review on the structural characteristics, antitumor mechanisms and immunomodulating activities. Carbohydr. Res. 424, 30–41.

Mondal, A., Bennett, L.L., 2016. Resveratrol enhances the efficacy of sorafenib mediated apoptosis in human breast cancer MCF7 cells through ROS, cell cycle inhibition, caspase 3 and PARP cleavage. Biomed. Pharmacother. 84, 1906–1914.

Nowacka, N., Nowak, R., Drozd, M., Olech, M., Los, R., Malm, A., 2014. Analysis of phenolic constituents, antiradical and antimicrobial activity of edible mushrooms growing wild in Poland. LWT (Lebensm.-Wiss. & Technol.) 59, 689–694.

Omidian, K., Rafiei, H., Bandy, B., 2017. Polyphenol inhibition of benzo[a]pyrene-induced oxidative stress and neoplastic transformation in an *in vitro* model of carcinogenesis. Food Chem. Toxicol. 106, 165–174.

Pal, M.K., Jaiswar, S.P., Srivastav, A.K., Goyal, S., Dwivedi, A., Verma, A., et al., 2016. Synergistic effect of piperine and paclitaxel on cell fate via cyt-c, Bax/Bcl-2-caspase-3 pathway in ovarian adenocarcinomas SKOV-3 cells. Eur. J. Pharmacol. 791, 751–762.

Pandurangan, M., Mistry, B., Enkhataivan, G., Kim, D.H., 2016. Efficacy of carnosine on activation of caspase-3 and human renal carcinoma cell inhibition. Int. J. Biol. Macromol. 92, 377–382.

Papetti, A., Maietta, M., Corana, F., Marrubini, G., Gazzani, G., 2017. Polyphenolic profile of green/red spotted Italian *Cichorium intybus* salads by RP-HPLC-PDA-ESI-MS. J. Food Compos. Anal. 63, 189–197.

Pawlaczyk-Graja, I., Balicki, S., Ziewiecki, R., Matulová, M., Capek, P., Gancarz, R., 2016. Polyphenolic-polysaccharide conjugates of *Sanguisorba officinalis* L. with anticoagulant activity mediated mainly by heparin cofactor II. Int. J. Biol. Macromol. 93, 1019–1029.

Pereira, J.M., Peixoto, V., Teixeira, A., Sousa, D., Barros, L., Ferreira, I.C.F.R., 2018. *Achillea millefolium* L. hydroethanolic extract inhibits growth of human tumor cell lines by interfering with cell cycle and inducing apoptosis. Food Chem. Toxicol. 118, 635–644.

Pires, T.C.S.P., Dias, M.I., Barros, L., Calhelha, R.C., Alves, M.J., Oliveira, M.B.P.P., et al., 2018. Edible flowers as sources of phenolic compounds with bioactive potential. Food Res. Int. 105, 580–588.

Pluchino, L.A., Liu, A.K., Wang, H.R., 2015. Reactive oxygen species-mediated breast cell carcinogenesis enhanced by multiple carcinogens and intervened by dietary ergosterol and mimosine. Free Radical Biol. Med. 80, 12–26.

Prados-Rosales, R., Toriola, S., Nakouzi, A., Chatterjee, S., Stark, R., Gerfen, G., et al., 2015. Structural characterization of melanin pigments from commercial preparations of the edible mushroom *Auricularia auricular*. J. Agric. Food Chem. 63, 7326–7332.

Rocha-Guzmán, N.E., Gallegos-Infante, J.A., González-Laredo, R.F., Reynoso-Camacho, R., Ramos-Gómez, M., Garcia-Gasca, T., et al., 2009. Antioxidant activity and genotoxic effect on HeLa cells of phenolic compounds from infusions of *Quercus resinosa* leaves. Food Chem. 115, 1320–1325.

Ruthes, A.C., Smiderle, F.R., Iacomini, M., 2016. Mushroom heteropolysaccharides: a review on their sources, structure and biological effects. Carbohydr. Polym. 136, 358–375.

Sergeeva, T.F., Shirmanova, M.V., Zlobovskaya, O.A., Gavrina, A.I., Dudenkova, V.V., Lukina, M.M., et al., 2017. Relationship between intracellular pH, metabolic cofactors and caspase-3 activation in cancer cells during apoptosis. BBA 1864, 604–611.

Stojković, D.S., Kovačević-Grujičić, N., Reis, F.S., Davidović, S., Barros, L., Popović, J., et al., 2017. Chemical composition of the mushroom *Meripilus giganteus* Karst. And bioactive properties of its methanolic extract. LWT (Lebensm.-Wiss. & Technol.) 79, 454–462.

Vallverdú-Queralt, A., Boix, N., Piqué, E., Gómez-Catalan, J., Medina-Remon, A., Sasot, G., et al., 2015. Identification of phenolic compounds in red wine extract samples and zebrafish embryos by HPLC-ESI-LTQ-Orbitrap-MS. Food Chem. 181, 146–151.

Wang, D., Lu, J., Miao, A., Xie, Z., Yang, D., 2008. HPLC-DAD-ESI-MS/MS analysis of polyphenols and purine alkaloids in leaves of 22 tea cultivars in China. J. Food Compos. Anal. 21, 361–369.

Wang, J., Zhang, Y., Thakur, K., Hussain, S.S., Zhang, J., Xiao, G., et al., 2018. Licochalcone A from licorice, an inhibitor of human hepatoma cell growth via induction of cell apoptosis and cell cycle arrest. Food Chem. Toxicol. 120, 407–417.

Wang, K., Zhang, Q., Liu, Y., Wang, J., Cheng, Y., Zhang, Y., 2013. Structural and inducing tumor cell apoptosis activity of polysaccharides isolated from *Lentinus edodes*. J. Agric. Food Chem. 61, 9849–9858.

Wang, L., Ding, L., Yu, Z., Zhang, T., Ma, S., Liu, J., 2016a. Intracellular ROS scavenging and antioxidant enzyme regulating capacities of corn gluten meal-derived antioxidant peptides in HepG2 cells. Food Res. Int. 90, 33–41.

Wang, L., Han, L., Ma, X., Yu, Q., Zhao, S., 2017. Effect of mitochondrial apoptotic activation through the mitochondrial membrane permeability transition pore on yak meat tenderness during postmortem aging. Food Chem. 234, 323–331.

Wang, L., Li, X.Y., Wang, Z.Y., 2016b. Whole body radioprotective effect of phenolic extracts from the fruits of *Malus baccata* (Linn.) Borkh. Food Funct. 7, 975–981.

Wu, X., Shen, Y., 2018. PMN inhibits colorectal cancer cells through inducing mitotic arrest and p53-dependent apoptosis via the inhibition of tubulin polymerization. Biochem. Bioph. Res. Co. 499, 927–933.

Xie, G., Wang, Z., Chen, Y., Zhang, S., Feng, L., Meng, F., et al., 2017. Dual blocking of PI3K and mTOR signalling by NVP-BEZ235 inhibits proliferation in cervical carcinoma cells and enhances therapeutic response. Cancer Lett. 388, 12–20.

Xie, J., Zhang, Y., Kong, D., Rexit, M., 2011. Rapid identification and determination of 11 polyphenols in Herba lycopi by HPLC-MS/MS with multiple reactions monitoring mode (MRM). J. Food Compos. Anal. 24, 1069–1072.

Xu, M., Kim, Y.S., 2014. Antitumor activity of glycerol via induction of cell cycle arrest, apoptosis and defective autophagy. Food Chem. Toxicol. 74, 311–319.

Yaguchi, K., Yamamoto, T., Shimada, M., Sugimoto, R., Nakamura, K., Ayabe, T., et al., 2018. Ploidy-dependent change in cyclin D2 expression and sensitization to ckd4/6 inhibition in human somatic haploid cells. Biochem. Bioph. Res. Co. 504, 231–237.

Zhang, L., Tu, Z., Wang, H., Fu, Z., Wen, Q., Chang, H., et al., 2015. Comparison of different methods for extracting polyphenols from *Ipomoea batatas* leaves, and identification of antioxidant constituents by HPLC-QTOF-MS. Food Res. Int. 70, 101–109.

Zhang, W., Feng, X., Alula, Y., Yao, S., 2017a. Bionic multi-tentacled ionic liquid-modified silica gel for adsorption and separation of polyphenols from green tea (*Camellia sinensis*) leaves. Food Chem. 230, 637–648.

Zhang, W., Zhu, Y., Liu, Q., Bao, J., Liu, Q., 2017b. Identification and quantification of polyphenols in hull, bran and endosperm of common buckwheat (*Fagopyrum esculentum*) seeds. J. Funct. Foods 38, 363–369.